Research, Society and Development, v. 9, n. 7, e789974669, 2020
(CC BY 4.0) | ISSN 2525-3409 | DOI: http://dx.doi.org/10.33448/rsd-v9i7.4669

Souza FM, Soares JMD, Oliveira HP, Rigoli IC & Luporini S (2020). Rheological assessment of the interaction between hydrophobic nanoclay and xanthan gum in saline environment, for application in drilling nanofluid. ***Research, Society and Development***, 9(7): 1-45, e789974669.

Avaliação reológica da interação entre nanoargila hidrofóbica e goma xantana em ambiente salino, para aplicação em nanofluido de perfuração

Rheological assessment of the interaction between hydrophobic nanoclay and xanthan gum in saline environment, for application in drilling nanofluid

Evaluación reológica de la interacción entre nanoargila hidrofóbica y goma xantana en un entorno salino para aplicación en nanofluidos de perforación

Recebido: 18/05/2020 | Revisado: 25/05/2020 | Aceito: 29/05/2020 | Publicado: 13/06/2020

Felipe Menezes de Souza
ORCID: https://orcid.org/0000-0002-6686-6320
Universidade Federal da Bahia, Brazil
E-mail: felipemenezessouza@gmail.com
Juliana Mikaelly Dias Soares
ORCID: https://orcid.org/0000-0003-2832-3461
Universidade Federal do Vale do São Francisco, Brazil
E-mail: juliana_mikaelly@hotmail.com.br
Helinando Pequeno de Oliveira
ORCID: https://orcid.org/0000-0002-7565-5576
Universidade Federal do Vale do São Francisco, Brazil
E-mail: helinando@gmail.com
Isabel Cristina Rigoli
ORCID: https://orcid.org/0000-0002-7042-2087
Universidade Federal da Bahia, Brazil
E-mail: irigoli@ufba.br
Samuel Luporini
ORCID: https://orcid.org/0000-0003-4334-5343
Universidade Federal da Bahia, Brazil
E-mail: sam5luporini@uol.com.br

Resumo

Na última década, a exploração em poços de altas temperatura e pressão tem motivado o aperfeiçoamento dos fluidos de perfuração com a aplicação de nanopartículas. Nesse contexto, as nanoargilas, as mais disponíveis das nanopartículas, tem sido aplicada no desenvolvimento de nanofluidos, principalmente associada a polímeros. Paralelamente, dos polímeros utilizados, a goma xantana tem sido pouco explorada para essa finalidade. Nesse trabalho foi avaliada, em solução, a interação entre a goma xantana, nanoargila hidrofóbica, cloreto de sódio e de cálcio e a influência destes sobre os parâmetros reológicos da mistura. Também foi avaliada a influência da temperatura e do tempo de hidratação sobre os parâmetros reológicos da mistura. Para tanto, primeiramente caracterirou-se a nanoargila com FRX, DRX e TGA. Em seguida, adotou-se um planejamento fatorial completo 2^4 variando as concentrações da nanoargila, xantana, cloretos de sódio e de cálcio. Em terceiro, adotou-se uma Matriz de Doehlert do tipo 7x5x3 variando as concentrações de nanoargila, xantana e temperatura, com as concentrações dos sais constantes. Em quarto, avaliou-se o efeito do tempo de hidratação sobre os parâmetros reológicos de amostras. Por fim, verificou-se Condutividade e Potenciais Zeta das amostras, variando a concentração dos componentes e o tempo de hidratação das misturas. Concluiu-se que as interações entre os componentes da mistura não estabilizam; a temperatura, os sais não exercem influência significativa sobre a reologia da mistura; a nanoargila em concentrações não superior a 5% (m/v) interage na Tensão de Cisalhamento Mínima; os parâmetros reológicos estabilizam após 96h de hidratação.

Palavras-chave: Nanoargila; Xantana; Nanofluido de perfuração; Reologia.

Abstract

In the last decade, exploration in high temperature and pressure wells has motivated the improvement of drilling fluids with the application of nanoparticles. In this context, nanoclay, the most available of nanoparticles, has been applied in the development of nanofluids, mainly associated with polymers. In parallel, among the polymers used, xanthan gum has been little explored for this purpose. In this work, the interaction between xanthan gum, hydrophobic nanoclay, sodium and calcium chloride and their influence on the rheological parameters of the mixture was evaluated in solution. The influence of temperature and hydration time on the rheological parameters of the mixture was also evaluated. For this purpose, nanoclay was first characterized with XRF, XRD

and TGA. Then, a complete factorial design 24 was adopted, varying the concentrations of nanoclay, xanthan, sodium and calcium chlorides. Third, a Doehlert Matrix of the 7x5x3 type was adopted, varying the concentrations of nanoclay, xanthan and temperature, with the concentrations of the constant salts. In the fourth, select the effect of the hydration time on the color rheological parameters. Finally, Conductivity and Potential Zetas of sizes were verified, varying the concentration of the components and the hydration time of the mixtures. It was concluded that the interactions between the components of the mixture do not stabilize; the temperature, the salts have no significant influence on the rheology of the mixture; nanoclay in concentrations not exceeding 5% (m/v) interacts with the Minimum Shear Stress; the rheological parameters stabilize after 96h of hydration.

Keywords: Nanoclay; Xanthan; Drilling Nanofluid; Rheology.

Resumen

En la última década, la exploración en pozos de alta temperatura y presión ha motivado la mejora de los fluidos de perforación con la aplicación de nanopartículas. En este contexto, la nanoarcilla, la más disponible de nanopartículas, se ha aplicado en el desarrollo de nanofluidos, principalmente asociados con polímeros. Al mismo tiempo, de los polímeros utilizados, la goma de xantano ha sido poco explorada para este propósito. En este trabajo, se evaluó en solución la interacción entre la goma de xantano, la nanoarcilla hidrófoba, el cloruro de sodio y calcio y su influencia en los parámetros reológicos de la mezcla. También se evaluó la influencia de la temperatura y el tiempo de hidratación en los parámetros reológicos de la mezcla. Para este propósito, la nanoarcilla se caracterizó por primera vez con FRX, DRX y TGA. Luego, se adoptó un diseño factorial completo 24, variando las concentraciones de cloruros de nanoarcilla, xantano, sodio y calcio. En tercer lugar, se adoptó una matriz Doehlert del tipo 7x5x3, variando las concentraciones de nanoarcilla, xantano y temperatura, con las concentraciones de las sales constantes. Cuarto, se evaluó el efecto del tiempo de hidratación sobre los parámetros reológicos de las muestras. Finalmente, se verificaron los potenciales de conductividad y Zeta de las muestras, variando la concentración de los componentes y el tiempo de hidratación de las mezclas. Se concluyó que las interacciones entre los componentes de la mezcla no se estabilizan; la temperatura, las sales no tienen influencia significativa en la reología de la mezcla; nano arcilla en concentraciones que no exceden

el 5% (m / v) interactúa con el esfuerzo de corte mínimo; Los parámetros reológicos se estabilizan después de 96 h de hidratación.

Palabras clave: Nanoarcilla; Xantano; Nanofluido de Perforación; Reología.

1. Introduction

With the increasing demand for oil in the world, oil drilling has gone into exploration in increasingly deep wells [Bland et al., 2006; Amanullah et al., 2011; EIA, 2017; Aftab, 2017]. For this drilling environment, under high pressures and temperatures, oil-based drilling fluids have historically been used [Caenn et al., 2014], however, the strengthening of environmental policies has directed the drilling industry towards the use of water-based fluids [Amanullah et al., 2011; Caenn et al., 2014]. Drilling in deep wells, in addition to being expensive [Fitzgerald et al., 2000], has limitations to the traditional water-based drilling fluids [Amanullah et al., 2011; Al-Yasiri and Al-Sallami, 2015], and to reverse this scenario, in the last decade, interest in the adoption of drilling nanofluids has grown [Amanullah et al., 2011; Fitzgerald et al., 2000; Perween et al., 2019; Al-Yasiri et al., 2019].

Drilling nanofluids are those that have some type of nanoparticle as an additive [Amanullah et al., 2011]. Nanoparticles are materials whose size varies from 1 to 100nm [Amanullah et al., 2011; EPA, 2010]. In the last decade, its their application has sought to mitigate problems caused in drilling with water-based fluids, for example, shale stability control [Al-Yasiri et al., 2019; Aftab et al., 2016; Parizad et al., 2018], filtrate control [Barry et al., 2015; Vryzas et al., 2015], improvement of rheological properties [Jain et al., 2015; Mao et al., 2015], improvement in thermal and electrical conductivity [Ponmani et al., 2014]. Moreover, the use of nanoparticles is economically interesting for drilling fluids, as it requires small amounts of additives to improve the desired property, and the improvement of the fluid results in a lower incidence of problems during operation and consequently shorter operating time [Amanullah et al., 2011].

In this scenario, nanoclay, the most widely used nanoparticles, having the greatest commercial application [Uddin, 2008], is interesting, mainly due to the vast availability of raw material and low production cost [Mélo et al., 2014]. The nano-montmorillonites come from the smectite family, have a laminar shape, with thickness of the order of 1 nm and length of the order of 10 μm [Golubeva, et al., 2013; Vipulanandan and Mohammed,

2015; Jain e Mahto, 2015]. Their applications are mainly aimed at obtaining nanocomposites, mostly because they are naturally hydrophilic, but susceptible, through substitution processes, made hydrophobic, which facilitates the interaction with polymers [Mélo et al., 2014; Santos et al., 2016; Amari and Sadeghialiabadi, 2014]. Their application goes through the area of drugs [Fejér et al., 2002; Viseras et al., 2010], biomedicine, catalysis and nanofiltration [Liu et al., 2011], biodegradable plastics [Yang et al., 2007], food [Slavutsky et al., 2012], civil construction [You et al., 2011], as well as in the development of drilling fluids. In this segment, Vipulanandan and Mohammed (2015) applied hydrophilic nanoclay to improve electrical and thermal conductivities and the rheological properties of fluids based on bentonite. Shakib et al. (2016) applied nanoclays together with other nanoparticles to control the filtration of bentonite-based sludge. Jain and Mahto (2015) applied nanoclays to form a polyacrylamide composite to inhibit shale. Abdo et al. (2013) produced and applied nano-bentonite in drilling fluid based on bentonite and cellulose to improve flow point, apparent viscosity and plastic viscosity. Abdo (2014) uses nano-attapulgite in commercial sludge to reduce friction between the drilling column and the well wall.

Abdo & Haneef (2013) use montmorillonite and nano-polygorskite in water to improve the rheological properties of the mixture. Abdo et al. (2016) uses nano-sepiolite to control filtrate in water-based sludge. Cheraghian et al. (2018) associated nanoclay and nanosilica to improve rheological properties and water-based fluid filtrate.

In parallel, the use of biopolymers in drilling fluids has been occurring since the second half of the 20th century [Caenn et al., 2014], mainly associated with improved filtrate control, well stability, emulsification, lubrication and improved rheological properties [Caenn et al., 2014; Rossi et al., 2003; Lucena et al., 2014], however, due to limitations for application at high pressure and temperature [Caenn et al., 2014; Sadeghalvaad and Sabbagui, 2015], in the last decade biopolymers have been modified by nanoparticles for the nanofluids development. Jain and Mahto (2015) associated polyacrylamide and nanoclay to control shale stability. Sadeghalvaad & Sabbaghi (2015) added titanium nano-oxide to polyacrylamide for improved filtrate and rheological properties. Aftab et al. (2016) added zinc nano-oxide in acrylamide to improve rheological parameters and filtrate control. Parizad et al. (2018) adds titanium nano-oxide to a mixture of xanthan gum (XG), hydrolyzed polyacrylamide, carboxymethylcellulose, and bentonite to enhance thermal and electrical conductivity, filtrate, shale stability and rheological properties. Ismail et al. (2016) added carbon nanotubes in a mixture of

polyanionic cellulose and hydrolyzed anionic polyacrylamide to improve rheological properties.

In this context, XG, a biopolymer added to drilling fluids since 1970 [Caenn et al., 2014; Kelco, 2000] still has great potential in the nanofluids development. Generally adopted as a fluid additive based on clay [Cheraghian, 2017] or in mixtures with other biopolymers [Parizad et al., 2018], its improvement by nanoparticles for the nanofluids development has been little explored. Srivatsa and Ziaja (2012) added nanosilica to XG solutions for filtrate control. Ponmani et al. (2014) applied copper nano-oxide and zinc nano-oxide to improve electrical and thermal conductivity. Perween et al. (2019) applied bismuth and iron nano-oxide to improve rheological properties and filtrate control.

Considering the physical and chemical properties of XG and its contribution, the properties of drilling fluids [Bland et al., 2006; Caenn et al., 2014; Lucena et al., 2014], and the versatility and availability of nanoclays and the improvement brought to the polymeric nanocomposites of this material [Uddin, 2008; Mélo et al., 2014; Santos et al., 2016; Amari and Sadeguialiabadi, 2014], the improving possibility the XG's characteristics with the nanoclay addition is interesting. In parallel, considering the interaction with shale and the nanometric dimensions of its pores [Khodja et al., 2010; Steiger & Leung, 1992; Chenevert, 1970; Al-Bazali et al., 2005; Cai et al., 2011], its inhibition demands anionic interactions, evaluated with the adoption of nanoparticles associated with polymers [Parizad et al., 2018; Jain & Mahto, 2015; Abdo e Haneef, 2013]. In this regard this work assesses the interaction between XG and hydrophobic montmorillonite (NA) nanoclay, in sodium chloride and calcium chloride solution. For this, were assesses the influence of the components of the mixture, temperature and time on the rheological parameters of the mixture, and the interaction between the components. As a methodology, were adopted two-level experimental planning with a central point, Response Surface Method [Ferreira, 2015] and evaluation of Electrical Conductivity and Zeta Potential [Rao et al., 2005; Shaw, 1992; Holmberg et al., 2002].

2. Methodology

This test was divided into five stages: in the first, NA was characterized by X-Ray Diffraction (XRD), X-Ray Fluorescence (XRD) and Thermogravimetry (TG); in the second, a complete factorial design 2^4 was carried out with three central points, varying the concentrations of NA, XG, and sodium and calcium salts; in the third, the

concentration of the salts was fixed, a Doehlert Matrix of the type 7x5x3 [Ferreira, 2015] was made, varying the concentrations of NA and XG, and the temperature; in the fourth, the hydration time's influence on the rheological parameters, using samples of equal concentrations for hydration times varying between 24h and 168h; fifth, the electrical conductivity and zeta potential tests were carried out on three samples with different concentrations of NA and XG and different rheological behaviors, and on samples whose concentration of the constant components, but subject to a hydration time varying between 24h and 168h.

Tables 1 and 2 show the components concentrations adopted in the experimental designs.

Table 1 – Complete factorial planning 2^4 with three central points.

Components	Concentrations (m/v)		
	-1	0	+1
NA	2,000%	3,000%	4,000%
XG	0,340%	0,510%	0,680%
NaCl	11,58%	12,86%	14,14%
$CaCl_2$	0,373%	0,414%	0,455%

Source: Authors.

Table 2 – Doehlert Matrix for three components.

NA (m/v)	NA Index	XG (m/v)	XG Index	Temperature (°C)	Temperature Index
5%	-1	0,17%	-1	25	-1
6%	-0.667	0,34%	-0.5	50	0
7%	-0.333	0,51%	0	75	+1
8%	0	0,68%	+0.5		
9%	+0.333	0,85%	+1		
10%	+0.667				
11%	+1				

Source: Authors.

Montmorillonite Nanoclay with modified surface with diethyl - dialkyl - 16, 18 - amine with a 35-45% m/m ratio by Sigma Aldrich (NA), the Xanthan Gum 200 MESH by Synth, Sodium Chloride PA (NaCl) by Synth and Calcium Chloride PA ($CaCl_2$) by Sigma Aldrich.

Tables 3 and 4 show the components concentrations in the mixture to assess the hydration time's influence and the hydration time intervals associated with each sample, respectively.

Table 3 – Mixture's composition for evaluation of the hydration time's influence in the mixture rheological behavior.

Components	Concentrations (m/v)
NA	8%
XG	0,51%
NaCl	12,86%
$CaCl_2$	0,414%

Source: Authors.

Table 4 – Simples and respective hydration times

Simples	Hydration Times (h)
1	168
2	144
3	120
4	96
5	72
6	48
7	24

Source: Authors.

To characterize the NA sample, an X-Ray Diffractometer, Shimadzu model XRD 7000, for the XRD assay, an X-Ray Fluorescence instrument of the Bruker model FRX S2 Ranger for the FRX test, and a thermogravimetric analyzer, Shimadzu model TGA-51-H for the TG test. The analytical balance of the brand BEL Engineering model S423, a mechanical stirrer of by Fisatom model 715 were used in all stages in the preparation of the samples and a mechanical stirrer by Hamilton Beach model 936 preceding the

viscosity tests. For the first stage and Fann viscometer, model 35A, and in the second stage the Haake viscometer.

For sample preparation, the components were added in the following sequence: distilled water was added to the beaker in 50% of the total sample volume; NA was added, and then the mixture was stirred between 1000 and 1500 rpm for 10 minutes. Then, XG was added, and the mixture was stirred between 1000 and 1500rpm for 10 minutes. Then, NaCl was added and the mixture was stirred at between 1000 and 1500 rpm for 5 minutes. Finally, $CaCl_2$ was added and the mixture was stirred at between 1000 and 1500 rpm for 5 minutes. The sample volume was completed with distilled water and then the sample was stirred for 1 minute. The samples were kept at 4°C for 24 hours and then analyzed. Preceding the analysis, they were stirred for 5 minutes.

To assess the components influence in the mixture, the rheological model most suitable for the system was first evaluated. Considering previous studies [Melo, 2008; Souza, 2016] and the thixotropy provided by NA and XG, the rheological models evaluated were pseudoplastic and Herschel-Bulkley.

To determine the most appropriate rheological model, non-linear regression of the results obtained on the viscometers was performed using the software *Origin Pro 2017*®. From the determination of the rheological parameters, the experimental results design were evaluated using the *STATISTICA 7*® software.

3. Results and Discussions

3.1. Part 1

The XRD test was performed with a copper anode at 40kV and a current of 45mA, with a step of 1.2°/min under continuous scanning. The results are shown in Figure 1.

Figure 1 – NA R-Ray Diagram.

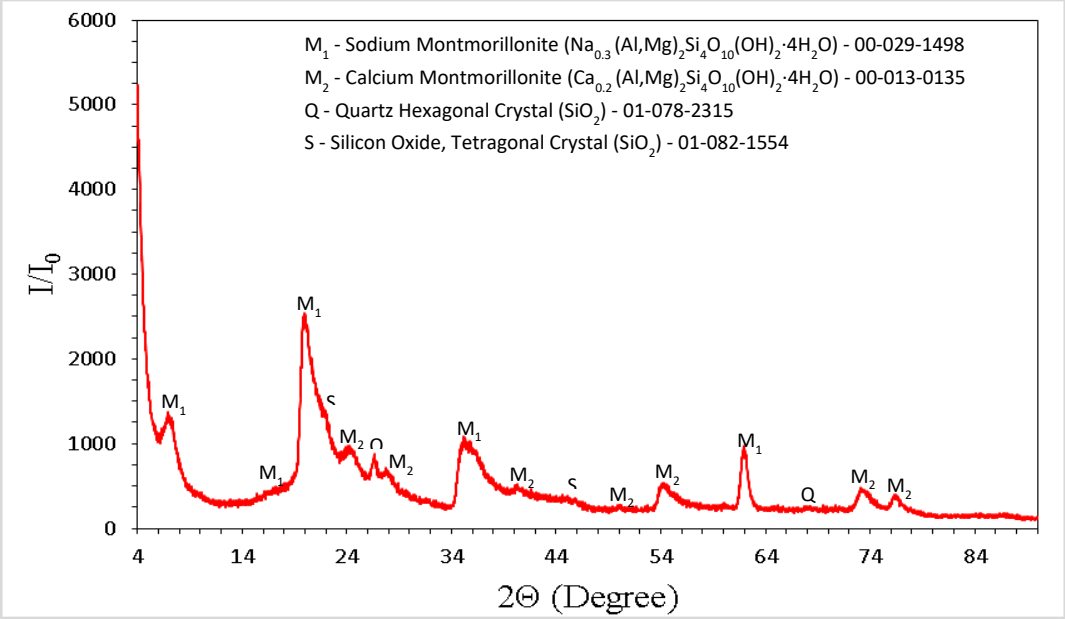

Source: Authors.

The XRD shows peaks at 20°, 34°, 54°, 62°, 73° and 75°, characteristic of Montmorillonite in the sodium and calcium forms, with a predominance of calcium in the presence of peaks 34°, 62°, 73° and 75°. The peaks between 20° and 30° are quartz and kaolinite residues [Morita et al., 2015; Paiva et al., 2008].

The main difference is perceived at peak 7°, which corresponds to the modification of interlayer spacing, which, in the evaluated sample, was 12.37Å, while in natural Montmorillonites it is of the order of 14.85Å at an angle of 5.95°.

This change in the diagram shows that the surfactant forms a lateral monolayer-like structure in the galleries (interlayer space of the clay lamellae) of the clay, corresponding to a concentration in the order of 0.2 to 0.5 times the clay's ion exchange capacity [Paiva et al., 2008; Xi et al., 2004].

This variation of approximately 1% may be associated with the formation of CO_2 and other gaseous species in the initial stages of surfactant degradation, but it is compensated by the release of surface water from the sample, which, even with less availability of exchangeable cations, is able to maintain adsorbed water [Xie et al., 2001].

The XRF is shown in Table 5. It is observed that the presence of sodium salts was not detected, which are in agreement with the replacement of the exchangeable ions of the clay in the order proposed by the previous analysis.

Table 5 – NA's X-Ray Fluorescence test.

Components	Amount (m/m)
MgO	3.70%
Al_2O_3	24.10%
SiO_2	66.68%
P_2O_5	0.12%
SO_3	0.24%
Cl	0.47%
K_2O	0.19%
CaO	0.15%
TiO_2	0.15%
Fe_2O_3	4.07%

Source: Authors.

Figure 2 shows the result of the clay thermogravimetry test. Initially, an increasing mass gain is observed between 21.36°C and 33.71°C, from 1,786mg to 1,803mg, then returns to the initial mass at 52.64°C.

Figure 2 – NA's Thermogravimetry test.

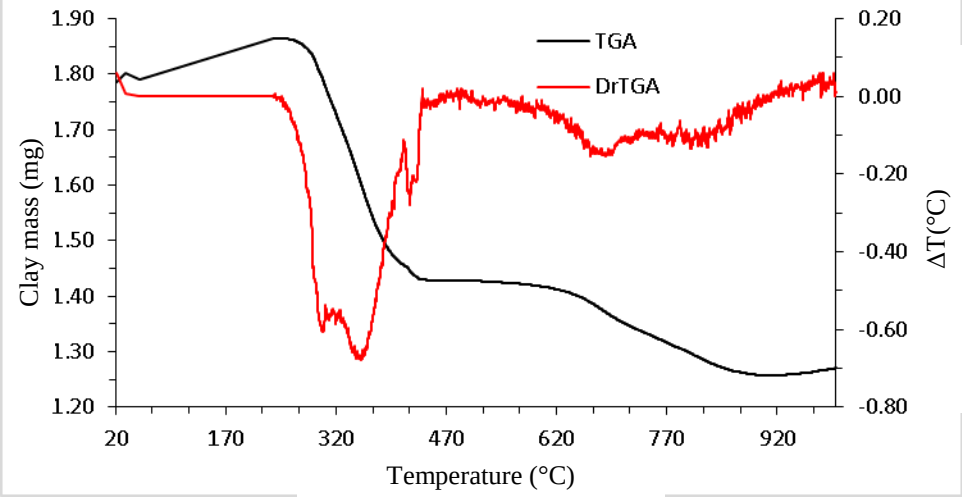

Source: Authors.

An increase in clay mass of approximately 4.12% is then observed, up to a temperature of 234.33°C, which can be justified by the balance of the loss of water physically absorbed by the clay, which occurs up to 180°C, melting of the surfactant and release of volatile species [Rossi et al., 2003], adsorption of CO_2 formed by the surfactant decomposition in itself [Planas et al., 2013] and the degradation's surfactant start, which starts after 200°C and stops until 400°C. After this interval, there is clay dehydroxylation - between 400°C and 600°C -, and residues oxidation of organic species - between 600°C and 1000°C [Xi et al., 2004; Xie et al., 2001].

3.2. Part 2

The objective of this step is to evaluate the influence that NA, XG, NaCl and $CaCl_2$ have on the rheological behavior of the mixture, individually or in an associated way. NA concentrations were selected considering that suspensions of microparticulate clay have non-Newtonian flow in concentrations equal to or greater than 3% by weight [Melo 2008; Luckham and Rossi, 1999], however, considering that samples with higher content of calcium ions as exchangeable cation for forming more bonds rigid with the clay lamellae making it difficult to hydrate [Santos, 2000; Abu-Jdayil, 2011], 4% was selected as the maximum value.

The minimum concentration was selected considering the XG contribution to the rheological behavior of the mixture: previous research has determined that 0.1% by weight stabilizes clay suspensions in saline environment [Xie and Lecourtier, 1992] and that adding 0.17% by weight of XG to clay suspensions at 2% by weight makes the mixture thixotropic [Melo, 2008].

Concentration of XG was determined considering that concentrations greater than 0.2% by mass, where the clay adopts the entangled regime, the rheology of the mixtures is favored by the addition of salt [Wyatt et al., 2011]. The critical concentration of NaCl and $CaCl_2$ were similar to Souza's work [Souza, 2016], with the aim of simulating the average concentration of salts incorporated into the mud during drilling in Brazilian shales.

At the same time, considering that XG and MMT are susceptible to precipitation in the presence of $CaCl_2$ [Santos, 2000; Xie and Lecourtier, 1992; Stawiński et al., 1990], the addition of 0.3% by XG weight is sufficient to stabilize suspensions with 3% by clay

weight in saline environment with up to 0.5% by $CaCl_2$ weight [Xie and Lecourtier, 1992].

It was also considered that NA, in its nanoparticulate state, has a larger surface area for interaction with XG [Helmy et al., 1999]. In this sense, it was also considered that XG interacts with alkylamines [Mukherjee et al., 2010], as well as the presence of cationic regions preserved in the clay lamellas, which would also enable the interaction between clay and anionic polymers in saline environment [Bailey and Keall, 1994; Benyounes et al., 2010].

The Matrix allows the evaluation of the concentration effects of the mixture components on the rheological parameters of the sample. As mentioned before, the flow models adopted are Pseudoplastic and Herschel-Bulkley. The previous models were adopted due to the greater rheological influence of XG in mixtures with clay [Benyounes et al., 2010]. First, the fit of the models to the flow was evaluated and, as shown in Table 6, the second model presents a more accurate R^2. Figure 3A shows the shear stress by shear rate, showing the rheological behavior of sample 1, treated with the Pseudoplastic model and Figure 3B shows the same graph treated with the Herschel-Bulkley model.

Figure 3 – Rheological behavior of sample 1 treated under a Pseudoplastic model (A) and treated under a Hershel-Bulkley model. (B)

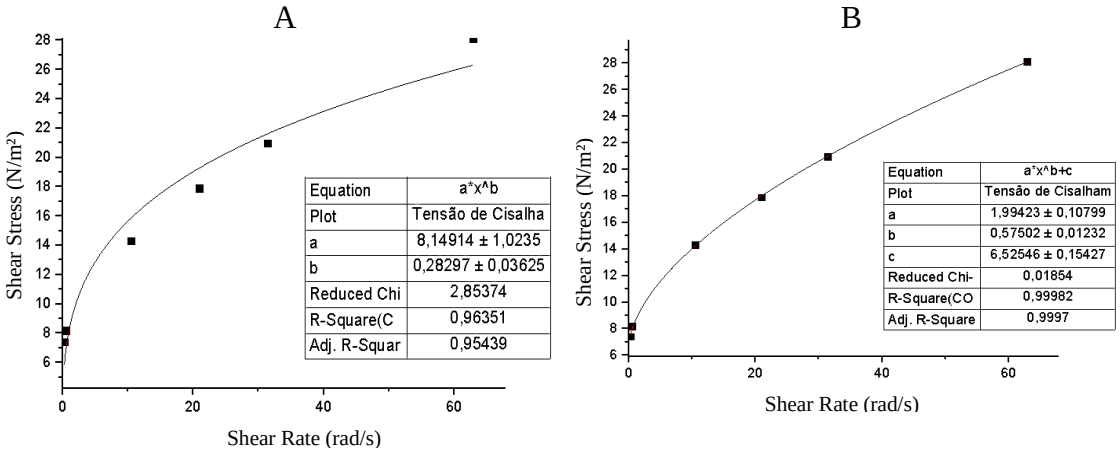

Source: Authors.

The rheological parameters of the Herschel-Bulkley model, as they are more accurate, were then analyzed using the Analysis of Variance (ANOVA) function of *STATISTICA 7*® with a 90% confidence interval. The analysis results of the experimental design for each parameter are presented in the Pareto Diagram of Figures 4A, 4B and 4C.

The ANOVA results are presented in Tables 7, 8 and 9, referring to the parameters Minimum Stress (τ_0), Consistency Index (k) and Behavior Index (n), respectively. The aforementioned tables present Quadratic Sum of Errors (SQ), Degrees of Release (GL), Quadratic Average of Errors (MQ), the values of Test F, the P Value, R^2 and adjusted R^2 [Calado and Montgomery, 2003].

Table 6 presents the Experimental Planning 2^4 Matrix with three central points applied to the experiment and the results obtained for the evaluated rheological parameters: Behavior Index (n), Consistency Index (k) and the flow Minimum Stress (τ_0). It also presents the Determination Coefficients (R^2) obtained by linear regression in the *Origin Pro 2017*® software for the adopted rheological models.

Table 6 – Factorial Planning 2^4 Matrix with three central points: the Pseudoplastic and Herschel-Bulkley models evaluation.

Samples	Components				Herschel-Bulkley Model				Pseudoplastic Model		
	GX	NA	NaCl	$CaCl_2$	k (Pa.s^n)	τ_0 (Pa)	n	R^2	k (Pa.s^n)	n	R^2
2	1	1	1	1	2.2630	8.8042	0.5810	0.9994	10.7258	0.2605	0.9570
3	1	-1	-1	1	2.2276	7.6138	0.5419	0.9999	9.6665	0.2461	0.9631
4	-1	1	-1	1	1.3637	3.6372	0.6051	0.9988	4.5261	0.3493	0.9703
6	1	-1	1	-1	2.9203	9.0535	0.5156	0.9999	11.8405	0.2381	0.9672
7	-1	1	1	-1	1.3053	2.9896	0.5709	0.9998	3.9709	0.3367	0.9752
8	-1	-1	-1	-1	1.4439	3.1322	0.5351	0.9999	4.3586	0.3070	0.9769
10	1	1	-1	-1	3.1880	10.3824	0.5059	0.9998	13.5142	0.2235	0.9666
11	-1	-1	1	1	1.1129	3.0047	0.5808	0.9999	3.8332	0.3207	0.9701
12	1	1	1	-1	2.8288	9.7883	0.5353	0.9998	12.4465	0.2388	0.9631
13	1	1	-1	1	2.9034	9.3104	0.5140	0.9997	12.1151	0.2320	0.9666
14	1	-1	1	1	2.9034	9.3104	0.5140	0.9997	12.1151	0.2320	0.9666
15	1	-1	-1	-1	2.9195	9.8267	0.5223	0.9997	12.6315	0.2321	0.9647
16	-1	1	1	1	1.2436	3.0443	0.5765	0.9997	3.9706	0.3319	0.9733
17	-1	1	-1	-1	1.1757	3.6237	0.6149	0.9997	4.3696	0.3351	0.9656
18	-1	-1	1	-1	1.1568	3.1170	0.5969	0.9995	3.9094	0.3384	0.9703
19	-1	-1	-1	1	1.1568	3.3727	0.5969	0.9995	4.1852	0.3248	0.9675
1	0	0	0	0	1.9942	6.5255	0.5750	0.9998	8.1491	0.2830	0.9635
5	0	0	0	0	1.7980	6.2642	0.5800	0.9998	7.7247	0.2777	0.9607
9	0	0	0	0	1.9662	6.2893	0.5563	0.9993	7.9987	0.2687	0.9647

Source: Authors.

Table 7 – Minimum Stress ANOVA (τ_0).

Variables	SQ	GL	MQ	Test F	F/F_0	P Value	R^2	R^2 Adjusted
(1)XG	145.0109	1	145.0109	827.5267	239.3148	0.000000	0.99068	0.97903
(2)NA	0.6199	1	0.6199	3.5374	1.0230	0.096786		
(3)NaCl	0.1996	1	0.1996	1.1393	0.3295	0.316947		
(4)$CaCl_2$	0.9100	1	0.9100	5.1931	1.5018	0.052165		
1 e 2	0.2054	1	0.2054	1.1719	0.3389	0.310564		
1 e 3	0.1284	1	0.1284	0.7328	0.2119	0.416876		
1 e 4	1.1070	1	1.1070	6.3174	1.8269	0.036176		
2 e 3	0.5139	1	0.5139	2.9326	0.8481	0.125162		
2 e 4	0.0016	1	0.0016	0.0091	0.0026	0.926229		
3 e 4	0.3154	1	0.3154	1.7996	0.5204	0.216593		
Error	1.4019	8	0.1752					
SQ Total	150.4140	18						

Source: Authors.

Table 8 – Consistency Index ANOVA (k).

Variables	SQ	GL	MQ	Test F	F/F_0	P Value	R^2	R^2 Adjusted
(1)XG	145.0109	1	145.0109	827.5267	239.3148	0.000000	0.99068	0.97903
(2)NA	0.6199	1	0.6199	3.5374	1.0230	0.096786		
(3)NaCl	0.1996	1	0.1996	1.1393	0.3295	0.316947		
(4)$CaCl_2$	0.9100	1	0.9100	5.1931	1.5018	0.052165		
1 e 2	0.2054	1	0.2054	1.1719	0.3389	0.310564		
1 e 3	0.1284	1	0.1284	0.7328	0.2119	0.416876		
1 e 4	1.1070	1	1.1070	6.3174	1.8269	0.036176		
2 e 3	0.5139	1	0.5139	2.9326	0.8481	0.125162		
2 e 4	0.0016	1	0.0016	0.0091	0.0026	0.926229		
3 e 4	0.3154	1	0.3154	1.7996	0.5204	0.216593		
Error	1.4019	8	0.1752					
SQ Total	150.4140	18						

Source: Authors.

Table 9 – Behavior Index ANOVA (n).

Variables	SQ[1]	GL[2]	MQ[3]	Test F	F/F0	P Value	R²	R² Adjusted
(1)XG	0.012507	1	0.012507	14.19974	4.10646	0.005479	0.67642	0.27195
(2)NA	0.000626	1	0.000626	0.71033	0.20542	0.423815		
(3)NaCl	0.000077	1	0.000077	0.08728	0.02524	0.775191		
(4)$CaCl_2$	0.000804	1	0.000804	0.91270	0.26395	0.367373		
1 e 2	0.000015	1	0.000015	0.01672	0.00484	0.900307		
1 e 3	0.000491	1	0.000491	0.55692	0.16106	0.476858		
1 e 4	0.000056	1	0.000056	0.06374	0.01843	0.807048		
2 e 3	0.000010	1	0.000010	0.01128	0.00326	0.918019		
2 e 4	0.000012	1	0.000012	0.01377	0.00398	0.909480		
3 e 4	0.000133	1	0.000133	0.15114	0.04371	0.707594		
Error	0.007046	8	0.000881					
SQ Total	0.021775	18						

Source: Authors.

Figure 4 – Pareto Diagram of the Minimum Stress - τ_0 - (A), Consistency Index - k - (B) and Behavior Index – n (C).

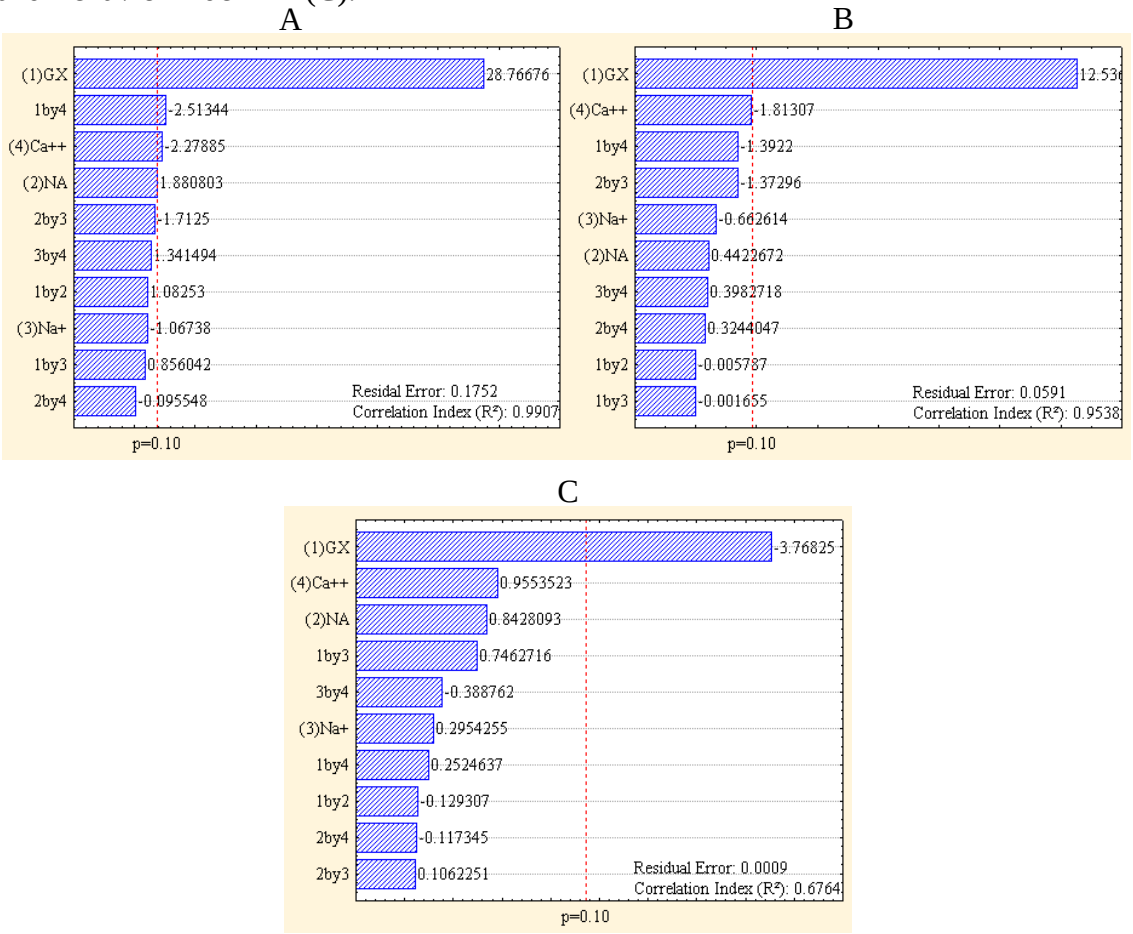

Source: Authors.

The ANOVA for Minimum Stress points to a good fit to the prediction model determined by the software, in addition to highlighting in red the variables that influenced the rheological parameter, in agreement with the Pareto of the respective. The relevant variables in the mixture were XG, NA, $CaCl_2$ and the interaction between XG and $CaCl_2$. As previously reported, XG exerts a significant influence on mixtures of XG with clays [Xie and Lecourtier, 1992; Benyounes et al., 2010], and XG and clays are sensitive to the presence of $CaCl_2$ [Santos, 2000; Xie and Lecourtier, 1992; Stawiński et al., 1990], however, unstable interaction between NA and XG was expected: historically, GX naturally interacts with the exchangeable cations in the environment [Wyatt and Liberatore, 2010; Zhong et al., 2013; Wyatt and Liberatore, 2009] and with the alkyne [Mukherjee et al., 2010], however the presence of surfactants on the faces of the clay lamellas certainly inhibited the interaction between the silanol groups of the clay [Rojtanatanya and Pongjanyakul, 2010; Rongthong et al., 2013] and the xanthan trisaccharides [Kelco, 2000], preventing the formation of hydrogen bonds [Rojtanatanya and Pongjanyakul, 2010; Rongthong et al., 2013]. It is also observed that the contribution of $CaCl_2$ is negative, either individually or with interaction with XG: both were expected, considering that this cation acts more strongly in stabilizing the anionic charges of the polymer, providing the screening of charges and consequent unraveling of the chains in double helix, making the macromolecules assume rod shapes and acquire a certain stiffness [Wyatt et al., 2011; Wyatt and Liberatore, 2010], however, considering XG concentrations greater than 0.2% by weight, the exposure of the polymer to the counterion should favor the viscosity before an expansion entanglement and consequent formation of hydrogen bonds [Wyatt and Liberatores, 2010; Zhong et al., 2013], which did not occur, demonstrating the interference of the other components in the interaction of XG with counterions.

Furthermore, NA's contribution to Minimum Stress is the smallest of the significant effects, being practically insignificant in view of XG's contribution, which encourages the discussion of its contribution to this specific parameter: Minimum Stress represents the flow resistance resulting from the formation of connections between particles dispersed in the environment, a characteristic of MMT, including that which provides thixotropy in suspensions of this material. It is worth remembering that XG, alone, does not present thixotropy [Kelco, 2000], however the mixture of this with clay provides this property to the environment, which allows to allude that XG assist the clays in the formation of the connection network between their particles through forces Van der

Walls and hydrogen bonds [Santos, 2000], but the origin of the property is of the clay. In this context, the results of ANOVA point to a minimum contribution of the property that is, theoretically, inherent to NA. This phenomenon can be justified by the presence of surfactant on the surface of the NA lamellae: due to their long carbon chain, decrease the polarity of the particles, interfering in their ability to form hydrogen bonds, certainly partially governing their interaction by Van der Walls forces, factors accentuated by the nanoparticulate state of the applied clay, which would hinder the interaction of the lamellae and consequent formation of the bonding particles network.

Figures 5A, 5B and 5C represent the interaction between the variables in the previous equation. By the figures, it is also possible to perceive the effect on the parameter discussed: in Figure 5A it is noticed that the Minimum Stress values are much more sensitive to the XG variation than the NA variation; this sensitivity to XG is repeated when comparing the effects of $CaCl_2$; Figure 5C shows that the effect of NA and $CaCl_2$ are similar on Minimum Stress, however the interaction range is small in comparison to the interactions of these variables, individually, with XG, showing the prevalence of the effects of the polymer on the parameter rheological.

Figure 5 – Interaction surface between τ_0, NA and XG (A); interaction surface between τ_0, Ca^{2+} e XG (B); Interaction surface between τ_0, Ca^{2+} e NA (C).

A

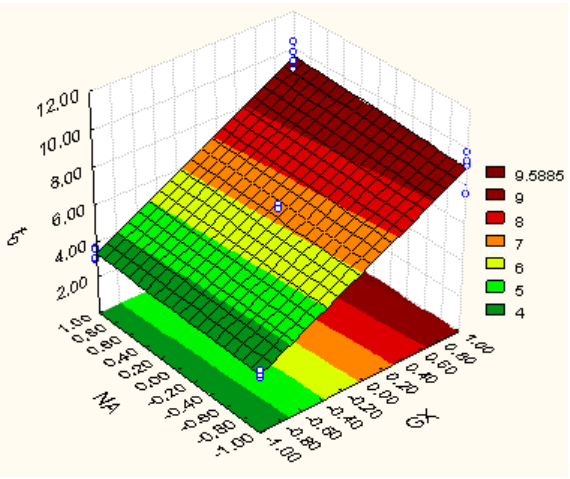

B

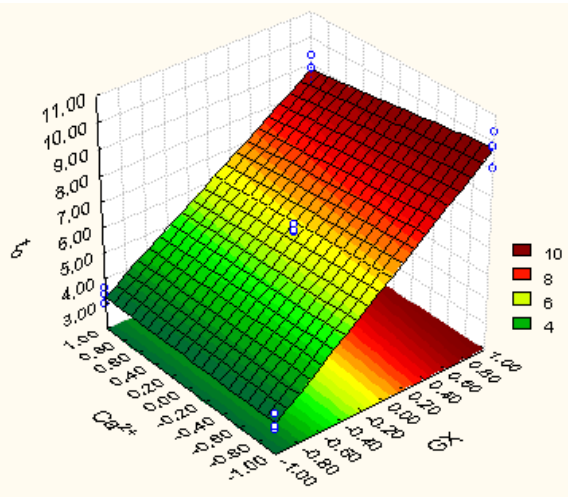

C

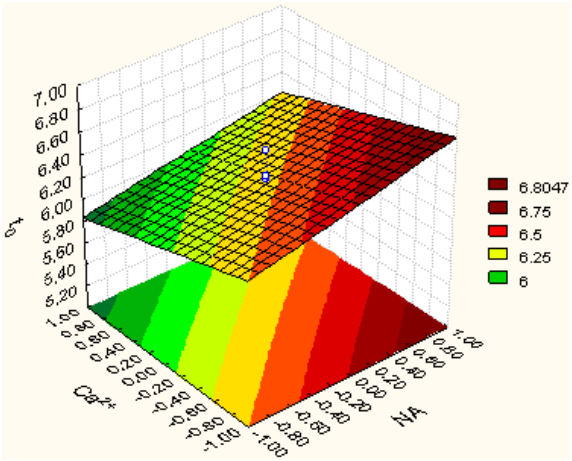

Source: Authors.

From the results obtained for ANOVA, one can consider the representation of the multiple variable linear regression model by Equation 1.

$$\tau_0 = 6.267896 + 3.010512 \cdot XG + 0.196831 \cdot NA - 0.238487 \cdot Ca^{2+} - 0.263038 \cdot XG \cdot Ca^{2+} \quad \text{Eq.(I)}$$

The ANOVA for the Consistency Index (k) also showed a good adjustment, as perceived by the adjusted R^2 and R^2. For this parameter, only XG's contribution was

detected. Recalling that, in mixtures of clay and XG, the rheological contribution of the polymer is predominant.

It is also observed that there was no contribution of NA to this parameter, as well as the counterions present in the environment. This can be justified considering that concentrations close to 6%, especially calcium clays, present Bingham Plastic rheology, offering greater resistance to the beginning of flow, but not to shear thinning, having an effective contribution to viscosity in higher concentrations [Abu-Jdayil, 2011].

XG, on the other hand, presents Newtonian viscosity in concentrations of the order of 20ppm [Holmberg et al., 2002], having its effect on viscosity very accentuated with the increase of its concentration in the environment. Therefore, considering that, in the mixture in question, the clay is nanoparticulated and in low concentration, it makes sense that the parameter in question has only a significant contribution from XG.

Another important consideration is that the electrolytes do not have a significant influence on the parameter, in contrast to the one presented in the Minimum Stress: in this case, it can be considered that the concentration of counterions has already exceeded the criticism [Wyatt and Liberatore, 2010], and therefore does not exert more influence on rheology. This contradiction allows us to conclude that XG interferes in fluid dynamics, but when in static, it has the function of assisting NA in the formation of particle networks.

Evaluating the fit of the models, only the Behavior Index showed a low R^2 and the adjusted R^2 to the reduced model compared to the previous one, meaning lack of predictive adjustment. However, considering that the values of this parameter are very close, with an average of 0.5589 and a standard deviation of the order of 6.554% of the average, it is concluded that this parameter is little affected by the system variables. In addition, for ANOVA it should be considered that such statistical treatment follows a Beta distribution [Quinino and Reis, 2011], therefore the R^2 associated with 90% reliability is 0.2473, which would make the data adjustment accurate.

3.3. Part 3

Given the significance of NA on the rheological parameters verified in the previous experimental design, plus the possibility of justifying this circumstance due to the low concentration of NA, since it was below the concentration in which it presents

thixotropy [Abu-Jdayil, 2011], a new experimental design was carried out to ascertain the effect of NA in higher concentrations.

It can then be admitted that this new range of NA concentration is a kind of "displacement" of the working range of the system in question, applied in order to resolve the doubt about the possibility of interactions between NA and the other components of the mixture, as also to evaluate the extent of its influence on the rheological parameters of the mixture.

In this scenery, it was decided to change the experimental planning model to the Response Surface (RSM), a methodology that allows the evaluation of the interaction between the input variables of the planning and its effects, individual or joint, on the output variable of the system, with greater "sensitivity" - for evaluating second order polynomial parameters - and greater "efficiency" - for requiring less experimental data [Ferreira, 2015; Calado and Montgomery, 2003; Montgomery, 2001]. For this methodology, the Doehlert Matrix was applied to plan the execution of the experiment, because, among the available ones, it presents a good accuracy with a smaller number of experiments [Ferreira, 2015; Ferreira et al., 2002; Verdooren, 2017; Sena et al., 2012].

For this stage, the salt concentrations were kept constant: the non-significant effect of NaCl in the previous stage was taken into account; the small effect of $CaCl_2$ on the system, mainly because it only presents statistical significance on the Minimum Stress; and, even more significant than the NA, this difference is around 20% between both, in addition to being less than 8% of the significance of XG.

In addition, the variation in concentration of these salts is approximately 10% in relation to the average of their concentrations in the environment, and the previous experiment suggests that the concentration range of the four components would not subject the mixture to clay flocculation [Santos, 2000; Xie and Lecourtier, 1992, Stawiński et al., 1990] or polymer precipitation [Xie and Lecourtier, 1992].

On the other hand, temperature was included as an input variable, which affects clays and polymer. The increase in temperature increases the flocculation of the clays, which allows a greater interaction between the lamellae released in the environment, enabling the formation of bonds between such particles and creating mechanical impediment by increasing these agglomerates, increasing the Minimum Stress of the clay suspensions and the viscosity, the latter increasing proportionally the shear rate applied on the system, making the behavior of suspensions more Newtonian, or in the context, closer to the Bingham model [Luckham and Rossi, 1999; Vryzas et al., 2016]; the

addition of NaCl and/or $CaCl_2$ favors the flocculation of the clay together with the increase in temperature, however the addition of XG in 0.1% by weight is sufficient to prevent the formation of precipitate at temperatures up to 125°C and 90°C, respectively [Xie and Lecourtier, 1992].

In parallel, XG solutions present a decrease in viscosity and approximation to Newtonian flow with an increase in temperature due to the change in conformation: XG in solutions without counterions, presents a helical conformation due to solvation and consequent repulsion of triglycerides, a phenomenon that favors the expansion of macromolecules, their separation into smaller structures and the formation of hydrogen bonds, however, given an anionic nature, the formation of a network of ligands has a weak interaction [Wyatt and Liberatore, 2009; Rocherfort and Middleman, 1987]; with increasing temperature, the helical structure changes to a coil structure [Rocherfort and Middleman, 1987] or disordered between the range of 47 to 51°C [Luporini and Bretas, 2011], which interferes with its rheology by decreasing its viscosity and making it more Newtonian [Benyounes et al., 2010; Speers and Tung, 1986], and when cooled, it changes its shape from disordered to fractured helix, which allows the formation of the network structure.

In the presence of counterions, this conformational transition does not occur in the temperature range adopted in this experiment, the helical structure remaining during heating and the fractured helix and consequent formation of a network with cooling [Wyatt and Liberatore, 2009; Luporini and Bretas, 2011].

Table 10 presents the Doehlert Matrix applied to the experimental planning of this stage.

Table 10 – Doehlert Matrix and rheological parameters for ANOVA.

Samples	XG	NA	T	k(Pa.s^n)	n	τ_0 (Pa)	R^2
2	0	-0.667	-1	0.2981	0.4844	4.6662	0.9987
7	-0.5	-1	-1	0.3656	0.4495	3.4358	0.9982
12	-0.5	0.333	-1	0.2189	0.4843	2.0751	0.9989
13	0.5	0.333	-1	0.3943	0.4870	9.4890	0.9994
1	0	0	0	0.6501	0.3917	5.6256	0.9985
3	1	0	0	2.8535	0.2608	11.0221	0.9958
6	-1	0	0	0.2244	0.4281	0.5876	0.9971
8	0.5	-1	0	0.3019	0.4880	10.0673	0.9994
16	-0.5	1	0	0.1845	0.5060	3.3057	0.9989
5 (0)	0	0	0	0.2217	0.5025	5.7466	0.9998
10 (0)	0	0	0	0.3503	0.4487	5.2995	0.9997
15 (0)	0	0	0	0.3874	0.4521	5.5825	0.9987
4	0	0.667	1	0.5937	0.3902	4.8197	0.9991
9	0.5	0.333	1	0.6160	0.3865	11.4505	0.9926
11	-0.5	-0.333	1	0.1995	0.4749	2.4911	0.9989
14	0.5	1	1	0.4336	0.4106	4.6087	0.9998

Source: Authors.

The concentrations corresponding to the levels adopted for the experiments are shown in Table 2. It is observed that the adjustment of the curves to the Herschel-Bulkey rheological model remains accurate.

It is also noticed that there are combinations of concentration and temperature that promote significant discrepancies for the evaluated rheological parameters. Tables 11, 12 and 13 show the results of ANOVA and Figures 6A, 6B and 6C show the Pareto Diagram of the Minimum Stress, Consistency Index and Behavior Index, respectively.

Table 11 – ANOVA by Doehlert Matrix for Minimum Stress (τ_0).

Variables	SQ	GL	MQ	Test F	F/F_0	P Value	R^2	R^2 Adjusted
(1)XG	1299143	1	1299143	37.56109	9.94732	0.000863	0.8690	0.67251
XG²	1680	1	1680	0.04856	0.01286	0.832894		
(3)NA	44961	1	44961	1.29993	0.34426	0.297685		
NA²	1392	1	1392	0.04024	0.01066	0.847640		
(3)T	3470	1	3470	0.10032	0.02657	0.762181		
T²	3425	1	3425	0.09904	0.02623	0.763646		
1 e 2	10831	1	10831	0.31314	0.08293	0.596016		
1 e 3	6678	1	6678	0.19307	0.05113	0.675755		
2 e 3	8375	1	8375	0.24214	0.06413	0.640149		
Error	207525	6	34587					
SQ Total	1584186	15						

Source: Authors.

Table 12 - ANOVA of the Doehlert Matrix for Consistency Index (k).

Variables	SQ	GL	MQ	Test F	F/F_0	P Value	R^2	R^2 Adjusted
(1)XG	20762.49	1	20762.49	8.092409	2.14312	0.029385	0.7497	0.3742
XG²	16870.20	1	16870.20	6.575347	1.74135	0.042664		
(3)NA	9.36	1	9.36	0.003649	0.00097	0.953793		
NA²	3354.23	1	3354.23	1.307346	0.34623	0.296436		
(3)T	193.45	1	193.45	0.075400	0.01997	0.792840		
T²	241.28	1	241.28	0.094042	0.02491	0.769463		
1 e 2	397.56	1	397.56	0.154953	0.04104	0.707454		
1 e 3	46.06	1	46.06	0.017951	0.00475	0.897799		
2 e 3	1982.68	1	1982.68	0.772771	0.20465	0.413178		
Error	15394.05	6	2565.67					
SQ Total	61494.49	15						

Source: Authors.

Figure 6 – Pareto Diagram of the Minimum Stress - τ_0 - (A), Behavior Index - n - (B) and Consistency Index - k - (C).

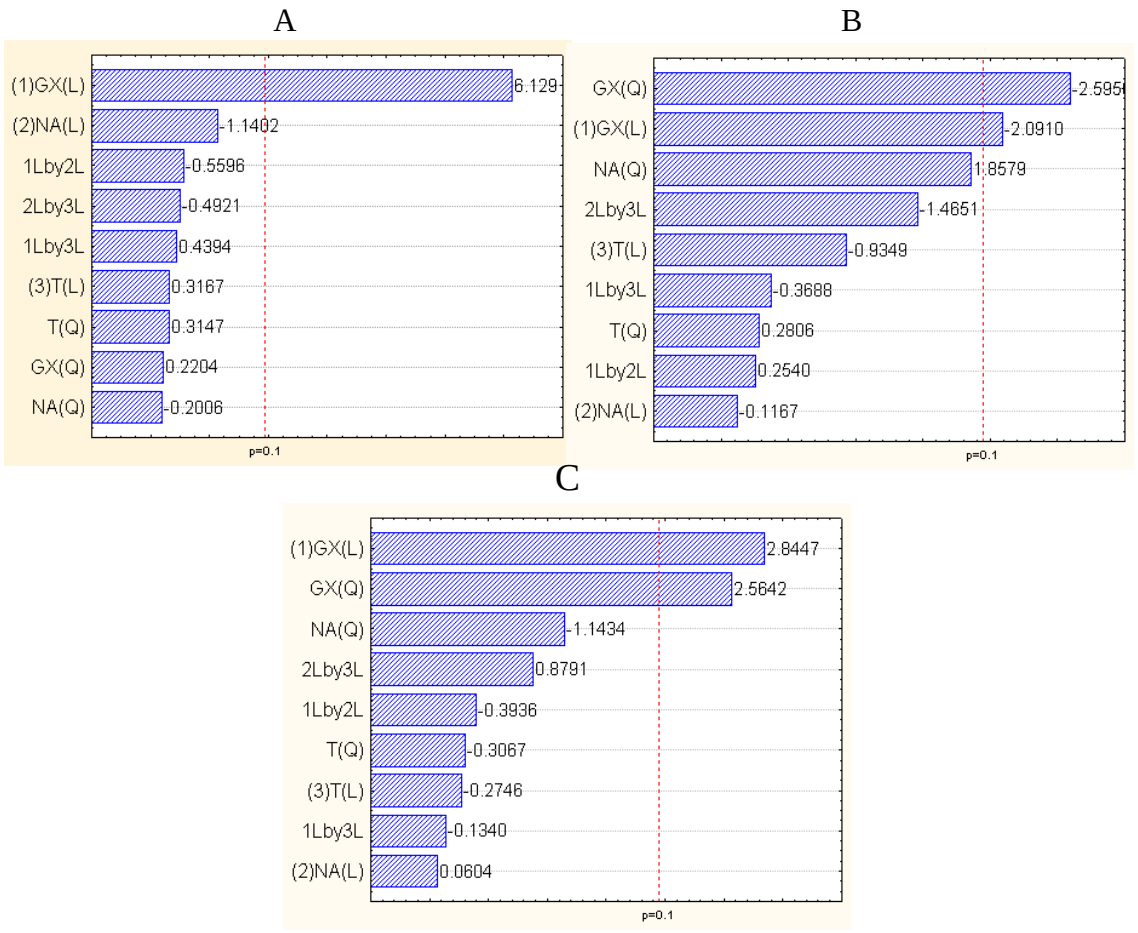

Source: Authors.

The Minimum Stress ANOVA shows accuracy with the RSM, as shown by the R^2 and the adjusted R^2, considering that this planning obeys a Beta type distribution [Quinino and Reis, 2011], with 0.3390 R^2 at 90% reliability. This rheological parameter,

however, before the increase in NA concentration for the evaluation of the polynomial model, only suffered significant influence from XG, even so under a linear effect, showing a proportionality relationship similar to the previous test, as ratified by the parameter Pareto Diagram.

On the other hand, the NA effect on the parameter is negative, that is, clay has contributed negatively on the rheological parameter, which contradicts previous studies that show a positive contribution to this rheological parameter, especially with the increase in the clay concentration in the suspension [Shakib et al., 2016; Abu-Jdayil, 2011; Bailey and Leall, 1994].

The verified effect can be justified by the presence of the surfactant which, in high concentrations of clay in the environment and consequent greater availability of lamellae with a larger substituted surface area, favors the electrostatic interaction between the particles and consequently in the formation of hydrogen bonds [Santos, 2000; Abu-Jdayil, 2011; Bailey and Leall, 1994], accentuated by the nanoparticulate state that would make the clay lamellae interaction and network formation difficult. However, it is observed that the p-value for NA under linear effect is the lowest after the p-value of XG, meaning a negative effect of organoclay for concentrations equal to or greater than 5% (m/v) and positive contributions to lower, as was even verified in the previous step.

The Minimum Stress does not present sensitivity to temperature variation, justified by the concentration of the salts present in the sample, what preserved XG from degradation [Xie and Lecourtier, 1992; Luporini e Bretas, 2011; Speers and Tung, 1986], as there is also possible early dissociation of NA sheets by the state particulate and, given the polarity promoted by the surfactant, interaction with the biopolymer [Benyounes et al., 2010] or the formation of the network, or even the flocculation of the clay with the increase in temperature [Xie and Lecourtier, 1992; Santos, 2000].

The Consistency Index ANOVA, considering the determination coefficient discussed above, is accurate when compared to its adjusted R^2 and R^2. This rheological parameter showed only sensitivity to XG, but it showed polynomial interaction, which allows us to affirm that the sensitivity of the parameter to variation in XG concentration is greater than that verified in the previous test. In addition, the contributions were positive, meaning that the increase in XG concentration contributes to the increase in the parameter [Ferreira, 2015].

This fact confirms previous research findings, confirming that XG exerts a greater influence on the viscosity of mixtures with clay [Xie and Lecourtier, 1992; Benyounes et al., 2010], as well as on the contribution to the formation of a network between the suspension particles and favoring the thixotropy promoted by clays and not by XG [Abu-Jdayil, 2011; Xie and Lecourtier, 1992]. NA does not have a significant effect on the parameter in question and has a negative contribution, meaning that increasing the concentration of NA in the environment ends up decreasing the parameter. The previous fact can be justified under the same analysis for Minimum Stress. The temperature also did not have a significant influence on this parameter, certainly due to the stability promoted by the concentration of sodium and calcium salts in the mixture [Xie and Lecourtier, 1992; Luporini e Bretas, 2011; Speers and Tung, 1986].

The Behavior Index also showed accuracy in terms of R^2 and adjusted R^2, both higher than required for the degree of freedom of planning. Similar to the previous parameter, only XG has a significant influence on the parameter, but this effect follows the polynomial model, which would imply greater sensitivity than that measured in the first planning. In addition, XG's contribution to the Behavior Index is negative, which means that increasing this component in the mix decreases the parameter in question, which is in line with previous research, which points to an increase in shear thinning with the increase the concentration of XG in solution [Wyatt and Liberatore, 2009; Speers and Tung, 1986].

The non-significant contribution of NA on the parameter was also expected, especially because the contribution of this component is more associated with resistance to initial flow and thixotropy, common to binghanian plastics, a flow model applied to clay suspensions at high concentrations [Luckham and Rossi, 1999;Vryzas et al., 2016]. The temperature does not significantly interfere with the parameter, confirming the theory that, for the concentration of salts and for the range adopted in this experimental stage, the non-degradation of the polymer [Xie and Lecourtier, 1992; Luporini e Bretas, 2011; Speers and Tung, 1986], as well as previous accentuated dispersion by the surfactant and state of aggregation.

Another important analysis is the quantification of the variables evaluated to optimize the rheological parameters [Ferreira, 2015; Montgomery, 2001]. In the perspective of the samples rheology, it is of primary interest that there is high viscosity to guarantee the dragging of gravel from the drilled well (Consistency Index), a high holding capacity of the gravel when the drilling is at rest (Minimum Stress) and a

thinning by shear when there is an increase in the fluid shear rate in the well, ensuring less mechanical stress on the equipment, greater penetrability in the reservoir rock, and greater ease in raising the fluid to the surface (Behavior Index) [Caenn et al., 2014; Abu-Jdayil, 2011; Vryzas et al., 2016].

In this scenario, observing Table 10, the XG influence is more significant: it is observed that sample 3, whose XG concentration in the mixture is the maximum (0.85% m/v), has the highest values of Minimum Stress and Consistency Index, even exposing the sample to 50°C; for sample 6, where the XG concentration was the lowest (0.17% m/v), the temperature and the NA concentration were the same as the previous one, there was a decrease of 92.14% in the Consistency Index and 94.67% in the Minimum Stress, in addition to an increase of 64.15% in the Behavior Index, meaning approximation to Newtonian behavior.

For Minimum Stress of samples 12 and 13, the NA concentration (8% m/v) and the temperature (25°C) are the same, however, with the increase in the XG concentration (from 0.34% to 0.68%) it promotes an increase of 357.28% over the parameter. The predominance of XG over the rheology of mixtures with clay was already foreseen [Xie and Lecourtier, 1992; Benyounes et al., 2010], however the absence of significant contribution from clay or temperature was not.

Another important discussion is at the Test Central Points, which reproduce as 5, 10 and 15. For these, the rheological tests presented a significant discrepancy, mainly for the Behavior Index - approximately 20% -, however it is important to consider those that were used by non-regressions linear and small differences, such as shear stresses, can justify changes in the calculated parameters given the propagation of errors [Montgomery, 2001].

Table 13 shows the shear stress values applied as three sizes. It is verified that the average measured for each voltage does not differ, but the mathematical adjustment indicates a significant discrepancy in the variables, especially for the Behavior Index. Figure 7A shows the shear stress rate curves for three colors mentioned and their average mean, and Figure 7B shows a curve with media stresses and the rheological parameters calculated from the average shear stresses.

Figure 7 – Rheological behavior (A) and Average Curve (B) of the Central Point samples.

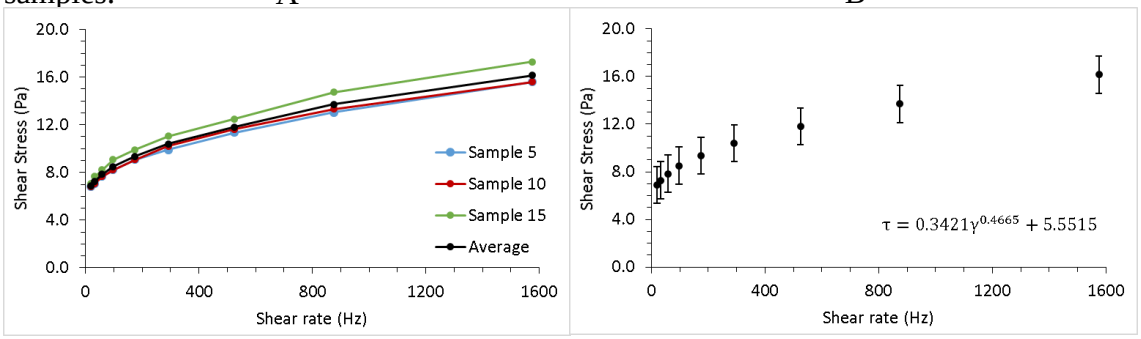

Source: Authors.

The Central Point of the experimental planning determines the variation of ANOVA [Ferreira, 2015; Montgomery, 2011], that is why the variance of these samples determines the accuracy of the results obtained.

The relevance of this information confirms a previous analysis, about the predominance of XG over the rheology of the mixture: these variables are determined by the central concentration measurement of the samples, and then, similarity to samples 3 and 6, maintains the statistics of NA and constant temperature and varies only XG.

Evaluates the average value used, observing the growth of the Minimum Stress between sample 3 (0.17% m/v) and the average of the central point (0.51%) of 167.53% and from this for sample 6 (0.86%) of 98.54%, confirming a previous theory.

Table 13 – Shear Stress average of the Central Points.

Shear Rate (Hz)	Shear Stress (Pa)			Average (Pa)	Standart D. (Pa)	Standart D. (%)	Confidence Interval (Pa)	
	Sample 5	Sample 10	Sample 15				Min. Value	Max. Value
19.44	6.804	6.804	7.088	6.899	0.1260	1.826%	6.839	6.958
32.40	7.088	7.088	7.655	7.277	0.2520	3.463%	7.158	7.395
58.32	7.655	7.655	8.222	7.844	0.2520	3.213%	7.725	7.962
97.20	8.222	8.222	9.072	8.505	0.3780	4.444%	8.327	8.683
174.96	9.072	9.072	9.923	9.356	0.3780	4.040%	9.177	9.534
291.60	9.923	10.206	11.057	10.395	0.4410	4.242%	10.187	10.603
524.90	11.340	11.624	12.474	11.813	0.4410	3.733%	11.605	12.020
874.80	13.041	13.325	14.742	13.703	0.6930	5.057%	13.376	14.029
1574.40	15.593	15.593	17.294	16.160	0.7560	4.678%	15.803	16.516

Source: Authors.

3.4. Part 4

For this experiment, according to Table 3, the levels of 8%, 0.51%, 12.86% and 0.414% (m/v) were used for NA, XG and storage and consumption salts, respectively; the test was carried out at 25°C. Melo (2008) lays down in his study that the XG establishes its rheological behavior by hydration of 24h, however MMT does not establish its rheological behavior in tests of up to 120h, which means that to have the possibility of alteration of this characteristic for evaluation tests superior to that studied by him.

For XG, in 24h, the rheological parameters become a more pseudoplastic mixture, for MMT, the rheological parameters become a more binghamian mixture that does not stabilize over 120h. This fact can be justified with the entry of water between the MMT crystalline layers, which allows both the swelling of the clay and consequent dissolution, as well as the formation of hydrogen bonds between them and the water, resulting in a gel effect [Santos, 2000; Abu-Jdayil, 2011]. Table 14 shows the variation in the Consistency Index, the Behavior Index and the Minimum Tension under the influence of the sample hydration time, respectively.

Table 14 – Influence of the Hydration Time on the Rheological Parameters of the Mixture.

Samples	Hydration Time (h)	k (Pa.s^n)	n	τ_0 (Pa)	R^2
7	24	0.2217	0.5025	5.7466	0.9998
6	48	0.5981	0.4336	7.8172	0.9992
5	72	0.4472	0.47151	8.1848	0.9996
4	96	0.4397	0.4585	6.1737	0.9991
3	120	0.4156	0.4693	6.6757	0.9996
2	144	0.3665	0.4797	6.5117	0.9992
1	168	0.3732	0.4780	6.7820	0.9986

Source: Authors.

Considering the parameter Consistency Index (k), which would mean an apparent viscosity of the environment [Caenn, 2014; Abu-Jdayil, 2011; Vryzas et al., 2016], it presents a growth of approximately 170%, that is, it almost triples between 24h and 48h of hydration. The previous phenomenon can be justified by the delay in hydration of XG

in the presence of NA, since its hydration time and consequent rheological stability is 24 hours when in distilled water [Melo, 2008; Xie and Lecourtier, 1992]. Another justification would be, considering the complete hydration of XG in 24h, a gradual hydration of NA, by the permeation of water molecules between the layers of NA [Xie et al., 2001; Santos, 2000], possible even in hydrophobic clays [Xie et al., 2001] and verified in step 1.

Additionally, the salt concentration, even considering the stability of the clay and XG mixture at the respective concentrations [Xie and Lecourtier, 1992], causes the clay flocculation fractions [Abu-Jdayil, 2011] and the biopolymer macromolecules separation into smaller and electrically stable fractions [Wyatt et al., 2011; Wyatt and Liberatore, 2010], which would justify the presence of dispersed particles in the environment and the consequent bonds formation between them, increasing the flow resistance. Subsequently, a drop of 25.23% is observed between 48h and 72h, still accentuated, but about 6.73 times less than the growth registered in the previous interval.

There is still a slight decrease in the parameter after 72h, with an amplitude of 19.75% between the observed values, under an average of 408.5 mPa.s^n, a standard deviation of 7.56%, the first value being 447.2mPa.s^n and the last, 373.2mPa.s^n. Therefore, it is possible to admit a certain stability after 72 hours of hydration, justified by a possible NA's continuous hydration and the consequent nanoparticles separation, resulting in less interaction between its crystals and a decrease in the gel effect in the system by breaking hydrogen bonds to a given limit, especially when evaluated against the parameters of the first interval.

Another justification would be the separation of the particles caused by the clay surfactant, which would interfere in the formation and maintenance of the polar bonds of the particles of the environment, however not so severe, as in an "accommodation" of the particles before the difference in polarity, justifying the smooth reduction to subsequent stabilization of the parameter values verified.

The Behavior Index (n) shows a very slight variation compared to the variation in the hydration time of the mixture, as shown in Figure 6b, with an average of 0.4704, standard deviation of 3.03%, and a maximum value of 0.5025 and a minimum of 0.4336, under a range of 14.65%. Therefore, one can consider a certain stability of this parameter over time, still guaranteeing the pseudoplasticity added by XG to the mixture [Wyatt and Liberatore, 2009; Speers and Tung, 1986], in addition to the predominant effect of XG on the rheological behavior of mixtures with clay [Xie and Lecourtier, 1992; Benyounes et

al., 2010]. In parallel, it is observed that the highest value for the parameter occurred in 24h of hydration of the mixture, which corroborates the delay in hydration of XG in the presence of NA or a gradual hydration of NA before the previous hydration of XG.

The Minimum Stress of the mixture showed a growth of 36% between 24h and 48h of hydration in the mixture, according to the previous phenomenological hypotheses. Then, there is a growth of 4.7% between 48h and 72h, and a reduction in the Consistency Index for the same interval, which allows us to conclude that the hydration effect of XG ends in 48h, remaining residually in NA. Then, there is a sharp drop in the value of the parameter (24.57%), under possible justification for separating the particles dispersed in the environment and reducing their interaction, either by hydration and consequent separation of the nanoclay lamellae, or by the presence of the surfactant, which prevents the formation of bonds between the faces of the clay lamellae.

The idea of the "accommodation" of the particles is corroborated with the parameters measured after 96h, which present an amplitude between minimum and maximum values of 9.31% in relation to the average, average of 6.5358 Pa and standard deviation of 2.95%. This phenomenon is in line with the trend of the other parameters, pointing to a stability of the components of the mixture after 96h of hydration.

3.5. Part 5

The previous results show that only GX and NA for concentrations below 5% (m/v) determine the rheological behavior in these mixtures. In addition, it was observed for samples of constant concentrations, that the hydration time affects the consistency index and the minimum tension of the mixture. To evaluate the interaction of the particles of the mixture subjected to the previous tests, Electrical Conductivity and Zeta Potential tests were adopted.

To evaluate the interaction of the components of the mixture subject to variation in concentration of GX and NA, samples 3, 10 and 12 were adopted: the first two were selected given the discrepancy in the values of the Consistency and Minimum Tension Indexes; already the sample 10, for being a central point of the test [Ferreira, 2015; Calado and Montgomery, 2003; Montgomery, 2001]. The concentrations of the respective samples, their rheological parameters, their Zeta Potential and Conductivity values are shown in Table 13.

To assess stability of the dispersions of the mixture over the hydration time, the Zeta Potential [Holmberg et al., 2008] and Conductivity [Rao et al., 2005; Shaw, 1992] were evaluated of the mixtures, the results of which are in Table 15. To assess the interaction of the components of the mixture subject to variation in the hydration time, the same samples as in the previous section were adopted. Table 16 presents the results of Electrical Conductivity and Zeta Potential measured for the hydration time from 24h to 168h.

The Conductivity values demonstrate a constant ion concentration in the environment [Rao et al., 2005; Shaw, 1992], that is, considering that the cations are adsorbed and desorbed by NA [Santos, 2000; Delgado et al., 1986] and XG [Caenn et al., 2014; Thonart et al., 1985], the stability of the conductivity results suggest that such a phenomenon has already reached equilibrium. The Zeta Potential values, which is a measure of dispersion stability [Holmberg et al., 2002], show significant variation, demonstrating that the particles are in frequent flocculation and deflocculation [Santos, 2000; Xie and Lecourtier, 1992], namely, that the colloidal structures are not stable. This is because the suspensions are considered stable when the Zeta Potential values are greater than ± 30mV [Salopek et al., 1992]. At the same time, MMT and XG, which form anionic suspensions, present when dispersed in water without additives, Zeta Potential values in the order of -20 to -70mV, and in the presence of mono, bi and trivalent cations, they end up varying their Zeta Potentials to values positive [Delgado et al., 1986; Thonart et al., 1985]. Therefore, the experimental results also point out that there is an unstabilized interaction between cations of NaCl and $CaCl_2$ and the particles of NA and XG, but not enough to make the suspensions stable.

Another relevant factor is that the biopolymer and nanoparticle concentrations do not affect the stability of the ions interactions in the environment: considering that the Electrical Conductivity points to availability of ions in the environment, it is observed that this quantity, regardless of the nature of the dispersed ion, the ion concentration is practically unchanged for the three samples. This perspective is confirmed by the results of Potential Zeta, which assesses the mobility of positive and/or negative ions in the environment, however the tests point to variations between positive and negative for the same sample, that is, the interactions between the dispersed ions do not stabilize.

Table 15 – Rheological Parameters, Zeta Potential and Electrical Conductivity of the samples 3, 10 e 12.

Samples	GX (m/v)	NA (m/v)	Temperature	k(Pa.s^n)	n	τ_0(Pa)	Zeta Potential (mV)			Condutividade (mS/cm)		
							Test 1	Test 2	Test 3	Test 1	Test 2	Test 3
3ª	0,85%	8.00%	50.0°C	2.8535	0.2608	11.0221	14.9	-33.5	25.3	157	156	156
10ª	0,51%	8.00%	50.0°C	0.3503	0.4487	5.2995	34.4	24.7	-13.9	151	151	151
12ª	0,34%	9.00%	25.0°C	0.2189	0.4843	2.0751	-29.2	-15.2	51.2	154	154	154

Source: Authors.

Table 16 - Potential zeta of the evaluated samples regarding the influence of the hydration time on the rheological behavior of the mixture with 8%, 0.51%, 12.86% and 0.414% (m/v) of NA, XG, NaCl and $CaCl_2$, respectively.

Samples	Hydration Time (h)	Zeta Potential (mV)			E. Conductivity (mS/cm)		
7	24	14.90	-33.50	25.30	157	156	156
6	48	3.38	12.90	2.76	163	162	162
5	72	-16.60	11.60	-18.50	164	162	163
4	96	19.80	-3.08	-31.00	163	162	162
3	120	11.80	44.60	-10.00	165	165	165
2	144	-5.64	-6.49	-2.72	166	166	166
1	168	3.34	-2.54	9.62	139	140	140

Source: Authors.

Similar to that observed for concentration variation, the results of Electrical Conductivity remain stable over the entire measurement period, meaning that the electrolytes concentration in the mixture practically does not vary over time [Rao et al., 2005; Shaw, 1992]. This demonstrates that the electrolytes concentration dispersed in the environment remains in balance for the entire interval of measurement time, showing that the hydration time does not influence the variation of electrolyte contraction and its consequent interactions with NA and XG. At the same time, it is observed that the values of Zeta Potential vary between positive and negative for triplicate measurements, demonstrating that there is a predominance of electrophoretic mobility, sometimes anionic, sometimes cationic, but that the interactions between the dispersed ions in the mixture do not stabilize [Salopek et al., 1992]. It is also noticed that, over the hydration

time, this transition remains, corroborating with the conclusion of the previous section, that the interactions between NA and XG with the salts dispersed in the environment do not stabilize over time. This means that the hydration time favors the stability of the interactions of the particles of the system [Santos, 2000; Abu-Jdayil, 2011].

4. Final Considerations

- The mixture rheological behavior is best described by the Herschel-Bulkley model.
- XG has a greater influence on the rheological parameters of the mixture with NA, as predicted by other authors. However, its effects are hegemonic compared to the other components. However, NA, even discreetly, has a linear influence on the Minimum Tension of the mixture, but in concentrations below 5% (m/v), as seen in the second experimental design.
- NaCl has not significant influence on the mixture. $CaCl_2$, on the other hand, influences the Minimum Stress of the mixture and presents interaction with XG, both negative effects, even under the polymer in a range of higher critical concentration [Wyatt and Liberatore, 2010].
- Temperature has not significant influence on mixtures, corroborating to preserve the helical structure of XG [Wyatt and Liberatore, 2009; Luporini and Bretas, 2011] and with stability of the rheological properties of mixtures of NA and XG in saline environment for the temperature range studied [Xie and Lecourtier, 1992].
- NA exerts an influence only on the Minimum Stress, as expected [Luckham and Rossi, 1999; Vryzas et al., 2016], with significance similar to that of $CaCl_2$. For concentrations equal to or greater than 5% (m/v), NA does not have a significant effect on the mixture, certainly due to the greater availability of surfactant in the environment, which should inhibit the interaction between XG and NA.
- The Zeta Potential results suggest that the interaction between the ions in the mixture does not stabilize. The variation in NA or XG concentration and the hydration time of the mixture did not affect the stability of the interactions.

References

Abdo J & Haneef MD (2013). Clay nanoparticles modified drilling fluids for drilling of deep hydrocarbon wells. *Appl. Clay Sci., 86,* 76–82. doi: 10.1016/j.clay.2013.10.017

Abdo J (2014). Nano-attapulgite for improved tribological properties of drilling fluids. *Surf. Interface Anal.*, 46, 882–887. doi: 10.1002/sia.5472

Abdo J, AL-Sharji H & Hassan E. (2016). Effects of nano-sepiolite on rheological properties and filtration loss of water-based drilling fluids. *Surf. Interface Anal., 48*(7), 522–526. doi: 10.1002/sia.5997

Abdo, M. I., Al-sabagh, A. M. & Dardir, M. M. (2013). Evaluation of Egyptian bentonite and nano-bentonite as drilling mud. *Egypt. J. Pet., 22*(1), 53–59. doi: 10.1016/j.ejpe.2012.07.002

Abu-Jdayil, B. (2011). Rheology of sodium and calcium bentonite–water dispersions: Effect of electrolytes and aging time. *Int. J. Miner. Process., 98*(3-4), 208–213. doi: 10.1016/j.minpro.2011.01.001

Aftab, A., Ismail, A. R., Ibupoto, Z. H., Akeiber, H. & Malghani, M. G. K. (2017). Nanoparticles based drilling muds a solution to drill elevated temperature wells: A review. *Renew. Sust. Energ. Rev., 76,* 1301–1313. doi: 10.1016/j.rser.2017.03.050

Aftab, A., Ismail, A. R., Khokhar, S. & Ibupoto, Z. H. (2016). Novel zinc oxide nanoparticles deposited acrylamide composite used for enhancing the performance of water-based drilling fluids at elevated temperature conditions. *J. Petrol. Sci. Eng., 146*, 1142–1157. doi: 10.1016/j.petrol.2016.08.014

Al-Bazali, T. M., Zhang, J., Chenevert, M. E. & Sharma, M. M. (2005, October 9-12). Measurement of the Sealing Capacity of Shale Caprocks. Paper presented at the *SPE Annual Technical Conference and Exhibition*. Dallas, TX: Society Petroleum Engineer. doi: 10.2118/96100-MS

Al-Yasiri, M. S. & Al-Sallami, W. T. (2015). How the Drilling Fluids Can be Made More Efficient by Using Nanomaterials. *Am. J. Nano Res. Appl., 3*(3), 41-45. doi: 10.11648/j.nano.20150303.12

Al-Yasiri, M., Awad, A., Pervaiz, S. & Wen, D. (2019). Influence of silica nanoparticles on the functionality of water-based drilling fluids. *J. Petrol. Sci. Eng., 179*, 504–512. doi: 10.1016/j.petrol.2019.04.081

Amanullah, M., Al-Arfaj, M. K. & Al-Abdullatif, Z. A. (2011, March 1-3). Preliminary test results of nano-based drilling fluids for oil and gas field application. Paper presented at the *SPE/IADC Drilling Conference and Exhibition*. Amsterdam: Society of Petroleum Engineers. doi: 10.2118/139534-MS

Amiri, C. & Sadeghialiabadi, H. (2014). Evaluating the Stability of Colloidal Gas Aphrons in the Presence of Montmorillonite Nanoparticles. *Colloid. Surface. A, 457*, 212-219. doi: 10.1016/j.colsurfa.2014.05.076

Bailey, L. & Keall, M. (1994). Effect of Clay Polymer Interactions on Shale Stabilization during Drilling. *Langmuir, 10*(5), 1544-1549. doi: 10.1021/la00017a037

Barry, M. M., Jung, Y., Lee, J. K. & Phuoc, T. X. (2015). Fluid filtration and rheological properties of nanoparticle additive and intercalated clay hybrid bentonite drilling fluids. *J. Petrol. Sci. Eng., 127*, 338–346. doi: 10.1016/j.petrol.2015.01.012

Benyounes, K., Mellak, A. & Benchabane, A. (2010). The Effect of Carboxymethylcellulose and Xanthan on the Rheology of Bentonite Suspensions. *Energ. Source. Part A, 32*, 1634–1643. doi: 10.1080/15567030902842244

Bland, R. G., Mullen, G. A., Gonzalez, Y. N., Harvey, F. E. & Pless, M. L. (2006, November 13-15). HP/HT Drilling Fluids Challenges. Paper presented at the *IADC/SPE Asia Pacific Drilling Technology Conference and Exhibition*. Bangkok: Society of Petroleum Engineers. doi: 10.2118/103731-MS

Caenn, R., Darley, H. C. H. & Gray, G. R. (2014). *Fluidos de Perfuração e Completação* (6 ed.). Rio de Janeiro, RJ: Elsevier.

Cai, J., Chenevert, M. E. & Friedheim, J. (2011, 30 October-2 November). Decreasing water Invasion into Atoka Shale Using Non-modified Silica Nanoparticles. Paper presented at the *SPE Annual Technical Conference and Exhibition*. Denver, CO: Society Petroleum Engineer. doi: 10.2118/146979-MS

Calado, V. & Montgomery, D. C. (2003). *Planejamento de Experimentos Usando Statistica*. Rio de Janeiro, RJ: E-paper Serviços Editoriais Ltda.

Chenevert, M. E. (1970). Shale Control with Balanced-Activity Oil-Continuous Muds. *J. Pet. Technol., 22*(10), 1309-1316. doi: 10.2118/2559-PA

Cheraghian, G. (2017). Application of Nano-Particles of Clay to Improve Drilling Fluid. *Int. J. Nanosci.. Nanotechnol., 13*(2), 177-186.

Cheraghian, G., Wu, Q., Mostofi, M., Li, M. C., Afrand, M. & Sangwai, J. S. (2018). Effect of a Novel Clay/silica Nanocomposite on Water-Based Drilling Fluids: Improvements in Rheological and Filtration Properties. *Colloid. Surface. A, 555*, 339-350. doi: 10.1016/j.colsurfa.2018.06.072

Delgado, A., Gonzalez-Caballero, F. & Bruque, J. M. (1986). On the Zeta Potential and Surface Charge Density of Montmorillonite in Aqueous Electrolyte Solutions. *J. Colloid Interf. Sci., 113*(1), 203-211. doi: 10.1016/0021-9797(86)90220-1

Energy Information Administration. (2017, September 14). *EIA projects 28% increase in world energy use by 2040*. Retrieved March 27, 2020, from https://www.eia.gov/todayinenergy/detail.php?id=32912.

Environmental Protection Agency. (2010, December 3). *Characteristics of Particles: Particle Size Categories.* Retrieved December 3, 2018, from http://www.epa.gov/apti/bces/module3/category/ category.htm.

Fejér, I., Kata, M., Erõs, I. & Dekany, I. (2002). Interaction of monovalent cationic drugs with montmorillonite. *Colloid. Polym. Sci., 280*(4), 37−379. doi: 10.1007/s00396-001-0619-2

Ferreira, S. L. C. (2015). *Introdução às Técnicas de Planejamento de Experimentos* (1 ed.). Salvador, BA: Vento Leste.

Ferreira, S. L. C., Santos, H. C., Fernandes, M. S. & Carvalho, M. S. (2002). Application of Doehlert matrix and factorial designs in optimization of experimental variables associated with preconcentration and determination of molybdenum in sea-water by inductively coupled plasma optical emission spectrometry. *J. Anal. At. Spectrom., 17*(2), 115–120. doi: 10.1039/B109087A

Fitzgerald, B. L., McCourt, A. J. & Brangetto, M. (2000, February 23-25). Drilling Fluid Plays Key Role in Developing the Extreme HTHP, Elgin/Franklin Field. Paper presented at the *IADC/SPE Drilling Conference*. New Orleans, LA: Society of Petroleum Engineers. doi: 10.2118/59188-MS

Golubeva, O. Y., Ul'yanova, N. Y., Kostyreva, T. G., Drozdova, I. A. & Mokeev, M. V. (2013). Synthetic Nanoclays with the Structure of Montmorillonite: Preparation, Structure, and Physico-Chemical Properties. *Glass Phys. Chem+, 39*(5), 533–539. doi: 10.1134/S1087659613050088

Helmy, A. K., Ferreiro, E. A. & Bussetti, S. G. (1999). Surface Area Evaluation of Montmorillonite. *J. Colloid Interfac. Sci., 210*(1), 167–171. doi: 10.1006/jcis.1998.5930

Holmberg, K., Shah, D. O. & Shwuger, M. J. (2002). *Handbook of applied surface and colloid chemistry* (pp.219-250). Chichester: Jonh Wiley e Sons Ltd.

Ismail, A. R., Aftab, A., Ibupoto, Z. H. & Zolkifile, N. (2016). The novel approach for the enhancement of rheological properties of water-based drilling fluids by using multi-walled carbono nanotube, nanosilica and glass beads. *J. Petrol. Sci. Eng., 139*, 264–275. doi: 10.1016/j.petrol.2016.01.036

Jain, R. & Mahto, V. (2015). Evaluation of polyacrylamide/clay composite as a potential drilling fluid additive in inhibitive water based drilling fluid system. *J. Petrol. Sci. Eng.*, *133*, 612–621. doi: 10.1016/j.petrol.2015.07.009

Jain, R., Mahto, V. & Sharma, V. P. (2015). Evaluation of polyacrylamide-grafted-polyethylene glycol/silica nanocomposite as potential additive in water based drilling mud for reactive shale formation. *J. Nat. Gas. Sci. Eng.*, *26*, 526–537. doi: 10.1016/j.jngse.2015.06.051

Kelco, C. Q. (2000). *Xanthan gum book* (8 ed.). Atlanta, GA: C. Q. Kelco.

Khodja, M., Canselier, J. P., Bergaya, F., Fourar, K., Khodja, M., Cohaut, N. & Bemounah, A. (2010). Shale problems and water-based drilling fluid optimisation in the Hassi Messaoud Algerian oil field. *Appl. Clay Sci.*, *49*(4), 383-393. doi: 10.1016/j.clay.2010.06.008

Liu, H., Nakagawa, K., Chaudhary, D., Asakuma, Y. & Tadé; M. O. (2011). Freeze-dried macroporous foam prepared from chitosan/xanthan gum/montmorillonite nanocomposites. *Chem. Eng. Res. Des.*, *89*(11), 2356–2364. doi: 10.1016/j.cherd.2011.02.023

Lucena, D. V., Lira, H. L. & Amorim, L. V. (2014). Efeito de aditivos poliméricos nas propriedades reológicas e de filtração de fluidos de perfuração. *Tecnol. Metal Mater. Miner.*, *11*(1), 66-73. doi: 10.4322/tmm.2014.010

Luckham, P. F. & Rossi, S. (1999). The colloidal and rheological properties of bentonite suspensions. *Adv. Colloid Interfac.*, *82*(1-3), 43–92. doi: 10.1016/S0001-8686(99)00005-6

Luporini, S. & Bretas, R. E. S. (2011). Caracterização Reológica da Goma Xantana: Influência de Íons Metálicos Univalente e Trivalente e Temperatura em Experimentos Dinâmicos. *Polímeros*, *21*(3), 188-194. doi: 10.1590/S0104-14282011005000043

Mao, H., Qiu, Z., Shen, Z. & Huang, W. (2015). Hydrophobic associated polymer based silica nanoparticles composite with core–shell structure as a filtrate reducer for drilling fluid at ultra-high temperature. *J. Pet. Sci. Eng., 129*, 1–14. doi: 10.1016/j.petrol.2015.03.003

Melo, K. C. (2008). *Avalição e modelagem reológica de fluidos de perfuração base água* (Master's Thesis). Universidade Federal do Rio Grande do Norte, Natal, RN.

Mélo, T. J. A., Araújo, E. M., Brito, G. F. & Agrawal, P. (2014). Development of nanocomposites from polymer blends: effect of organoclay on the morphology and mechanical properties. *J. Alloy Compd., 615*, S391-S391. doi: 10.1016/j.jallcom.2013.11.151

Montgomery, D.C. (2001). *Design and analysis of experiments* (5 ed., pp.590-629). New York, NY: John Wiley & Sons.

Morita, R. Y., Barbosa, R. V. & Kloss, J. R. (2015). Caracterização de Bentonitas Sódicas: Efeito do Tratamento com Surfactante Orgânico Livre de Sal de Amônio. *Rev. Virtual Quim.,7*(4),1286-1298. doi: 10.5935/1984-6835.20150071

Mukherjee, I., Sarkar, D. & Moulik, S. P. (2010). Interaction of Gums (Guar, Carboxymethylhydroxypropyl Guar, Diutan, and Xanthan) with Surfactants (DTAB, CTAB, and TX-100) in Aqueous Medium. *Langmuir, 26*(23), 17906–17912. doi: 10.1021/la102717v

Paiva, L. B., Morales, A. R. & Díaz, F. R. V. (2008). Argilas organofílicas: características, metodologias de preparação, compostos de intercalação e técnicas de caracterização. *Ceramica*, 54(330), 213-226. doi: 10.1590/S0366-69132008000200012.

Parizad, A., Shahbazi, K. & Tanha, A. A. (2018). Enhancement of polymeric water-based drilling fluid properties using nanoparticles. *J. Petrol. Sci. Eng., 170*, 813–828. doi: 10.1016/j.petrol.2018.06.081

Perween, S., Thakur, N. K., Beg, M., Sharma, S. & Ranjan, A. (2019). Enhancing the properties of Water based Drilling Fluid using Bismuth Ferrite Nanoparticles. *Colloid. Surface. A, 561*, 165-177. doi: 10.1016/j.colsurfa.2018.10.060

Planas, N., Dzubak, A. L., Poloni, R., Lin, L. C., McManus, A., McDonald, T. M., … Gagliardi, L. (2013). The Mechanism of Carbon Dioxide Adsorption in an Alkylamine – Functionalized Metal-Organic Framework. *J. Am. Chem. Soc., 135*(20), 7402-7405. doi: 10.1021/ja4004766

Ponmani, S., William, J. K. M., Samuel, R., Nagarajan, R. & Sangwai, J. S. (2014). Formation and characterization of thermal and electrical properties of CuO and ZnO nanofluids in xanthan gum. *Colloid. Surface. A, 443*, 2014, p.37–43. doi: 10.1016/j.colsurfa.2013.10.048

Quinino, R. C. & Reis, E. A. (2011). *O Coeficiente de Determinação R^2 como Instrumento Didático para Avaliar a Utilidade de um Modelo de Regressão Linear Múltipla*. Retrieved December 29, 2018, from http://www.est.ufmg.br/ portal/arquivos/rts/PD_28102011_Final.pdf.

Rao, M. A., Rizvi, S. S. H. & Datta, A. K. (2005). *Engineering Properties of Foods* (3 ed, pp. 461-500). Boca Raton, FL: Taylor and Francis Group.

Rochefort, W. E. & Middleman, S. (1987). Rheology of Xanthan Gum: Salt, Temperature, and Strain Effects in Oscillatory and Steady Shear Experiments. *J. Rheol., 31*, 337-369. doi: 10.1122/1.549953

Rossi, S., Luckham, P. F. & Tadros, T. F. (2003). Influence of non-ionic polymers on the rheological behaviour of Na-montmorillonite clay suspensions. Part II. Homopolymer ethyleneoxide and polypropylene oxide/ polyethylene oxide ABA copolymers. *Colloid. Surface. A, 215*(1-3), 1-10.

Sadeghalvaad, M & Sabbaghi, S. (2015). The Effect of the TiO2/Polyacrylamide Nanocomposite on Water-Based Drilling Fluid Properties. Powder Technol., 272, 113–119. doi: 10.1016/j.powtec.2014.11.032

Salopek, B., Krasić, D. & Filipović, S. (1992). Measurement and application of zeta-potential. *Rud.-geol.- naft. zb., 4*, 147-151.

Santos, P. S. (2000). *Tecnologia das Argilas: Fundamentos* (Vol. 1). São Paulo, SP: Edgard Blücher.

Santos, R. F. A., Reis, M. M., Ueki, M. M., Santos, Z. I. G. & Brito, G. F. (2016, November 6-10). Influência da argila montmorilonita nas propriedades mecânicas e morfológicas de nanocompósitos obtidos a partir de blendas de polietileno/poli (tereftalato de etileno). Paper presented at the *22º Congresso Brasileiro de Engenharia e Ciência dos Materiais*. Natal, RN: Associação Brasileira de Cerâmica.

Sena, A. R., Valasques Júnior, G. L., Barretto, I. K. S. P. & Assis, S. A. (2012). Application of Doehlert experimental design in the optimization of experimental variables for the Pseudozyma sp. (CCMB 306) and Pseudozyma sp. (CCMB 300) cell lysis. *Ciênc. Tecnol. Aliment.*[online], *32*(4), 762-767. doi: 10.1590/S0101-20612012005000118.

Shakib, J. T., Kanani, V. & Pourafshary, P. (2016). Nano-clays as additives for controlling filtration properties of water - bentonite suspensions. *J. Petrol. Sci. Eng., 138*, 257-264. doi: 10.1016/j.petrol.2015.11.018

Shaw, D. J. (1992). *Colloid and Surface Chemistry* (4 ed., pp.174-243). Oxford: Elsevier Science Ltd.

Slavutsky, A. M., Bertuzzi, M. A. & Armada, M. (2012). Water barrier properties of starch-clay nanocomposite films. *Braz. J. Food. Technol., 15*(3), 208-218. doi: 10.1590/S1981-67232012005000014

Souza, G. S. (2016). *Caracterização reológica de dispersões argilosas com goma xantana para fluidos de perfuração de poços de petróleo* (Master's Thesis). Universidade Federal da Bahia, Salvador, BA.

Speers, R. A. & Tung, M. A. (1986). Concentration and Temperature Dependence of Flow Behavior of Xanthan Gum Dispersions. *J. Food Sci., 51*(1), 96-98. doi: 10.1111/j.1365-2621.1986.tb10844.x

Stawiński, J., Wierzchoś, J. & Garoa-Gonzalez, M.T. (1990). Influence of Calcium and Sodium Concentration on the Microstructure of Bentonite and Kaolin. *Clay. Clay Miner, 38*, 617–622. doi: 10.1346/CCMN.1990.0380607

Steiger, R. P. & Leung, P. K. (1992). Quantitative Determination of the Mechanical Properties of Shales. *SPE Drilling Engineering, 7*(3), 181-185. doi: 10.2118/18024-PA

Thonart, Ph., Paquot, M., Hermans, L. & Alaoui, H. (1985). Xanthan production by Xanthomonas campestris NRRL B-1459 and interfacial approach by zeta potential measurement. *Enzyme Microb. Technol.,* 7(5), 235-238. doi: 10.1016/S0141-0229(85)80009-0

Uddin, F. (2008). Clays, Nanoclays, and Montmorillonite Minerals. *Metall. Mater. Trans. A Phys. Metall. Mater. Sci., 39*(A), 2804-2814.

Verdooren, L. R. (2017). Use of Doehlert Designs for Second-order Polynomial Models. Mathematics and Statistics, 5(2), 62-67. doi: 10.13189/ms.2017.050202

Vipulanandan, C. & Mohammed, A. (2015). Effect of nanoclay on the electrical resistivity and rheological properties of smart and sensing bentonite drilling muds. *J. Petrol. Sci. Eng., 130*, 86-95. doi: 10.1016/j.petrol.2015.03.020

Viseras, C., Cerezo, P., Sanchez, R., Salcedo, I. & Aguzzi, C. (2010). Current challenges in clay minerals for drug delivery. *Appl. Clay Sci., 48*(3), 291–295. doi: 10.1016/j.clay.2010.01.007

Vryzas, Z., Mahmoud, O., Nasr-El-Din, H. A. & Kelessidis, V. C. (2015). Development and testing of novel drilling fluids using Fe2O3 and SiO2 nanoparticles for enhanced drilling operations. *J. Pet. Technol., 68*(11), 48-50. doi: 10.2118/1116-0048-JPT

Vryzas, Z., Wubulikasimu, Y., Gerogiorgis, D. I. & Kelessidis, V. C. (2016). Understanding the Temperature Effect on the Rheology of Water-Bentonite Suspensions. *Annual Transactions - The Nordic Rheology Society*, *24*, 199-208.

Wyatt, N. B & Liberatore, M. W. (2010). The effect of counterion size and valency on the increase in viscosity in polyelectrolyte solution. *Soft Matter, 6*(14), 3346–3352. doi: 10.1039/C000423E

Wyatt, N. B. & Liberatore, M. W. (2009). Rheology and Viscosity Scaling of the Polyelectrolyte Xanthan Gum. *J. Appl. Polym. Sci., 114*, 4076–4084. doi: 10.1002/app.31093

Wyatt, N. B., Gunther, C. M. & Liberatore, M. W. (2011). Increasing viscosity in entangled polyelectrolyte solutions by the addition of salt. *Polymer, 52*(11), 2437-2444. doi: 10.1016/j.polymer.2011.03.053

Xi, Y., Ding, Z., He, H. & Frost, R. L. (2004). Structure of organoclays - an X-ray diffraction and thermogravimetric analysis study. J. *Colloid Interf. Sci., 277*(1), 116-120. doi: 10.1016/j.jcis.2004.04.053

Xie, W. & Lecourtier, J. (1992). Xanthan behavior in water-fluid drilling fluids. *Polym. Degrad. Stabil., 38*(2), 155-164.

Xie, W., Gao, Z., Pan, W. P., Hunter, D., Singh, A. & Vaia, R. (2001). Thermal Degradation Chemistry of Alkyl Quaternary Ammonium Montmorillonite. *Chem. Mater., 13*(9), 2979-2990. doi: 10.1021/cm010305s

Yang, K. K., Wang, X. L. & Wang, Y. Z. (2007). Progress in Nanocomposite of Biodegradable Polymer. *J. Ind. Eng. Chem., 13*(4), 485-500.

You, Z., Mills-Beale, J., Foley, J. M., Roy, S., Odegard, G. M., Dai, Q. & Goh, S. W. (2011). Nanoclay-modified asphalt materials: Preparation and characterization. *Constr. Build. Mater., 25*(2), 1072–1078. doi: 10.1016/j.conbuildmat.2010.06.070

Zhong, L., Oostrom, M., Truex, M. J., Vermeul, V. R. & Szecsody, J. E. (2013). Rheological behavior of xanthan gum solution related to shear thinning fluid delivery for subsurface remediation. *J. Hazard. Mater.*, *244–245*, 160–170. doi: 10.1016/j.jhazmat.2012.11.028

Percentage contribution of each author in the manuscript

Felipe Menezes de Souza – 50%

Juliana Mikaelly Dias Spares – 15%

Helinando Pequeno de Oliveira – 15%

Isabel Cristina Rigoli – 10%

Samuel Luporini – 10%